Temperature-Dependent Pyrolysis of Wood Chips in a Fixed-Bed Reactor: Effects on Syngas and Charcoal Yield and Quality

V.V. Badenko[1,*], M.V. Penzik[1], E.V. Gubiy[1], A.N. Kozlov[1]

[1] Melentiev Energy Systems Institute of Siberian Branch of Russian Academy of Sciences, Irkutsk, Russia

***Abstract* — In the context of the global challenge of reducing greenhouse gas and pollutant emissions from thermal and power generation systems, the utilization of secondary fuels, particularly biomass waste, is gaining increasing importance. A promising approach is the thermochemical conversion of wood waste via pyrolysis, which enables the production of energy carriers (syngas and charcoal) with minimal environmental impact. This paper presents a series of various experiments conducted with wood chips at temperatures ranging from 360 to 520 °C. The optimal pyrolysis temperature is found to be 480 °C, resulting in the highest syngas heating value of 12.69 MJ/m³, mechanical gas efficiency of 84.9%, and cold gas efficiency of 25.8 %. The findings also reveal that as temperature increases, charcoal yield decreases from 36% to 27.5%, gas yield rises from 11.1% to 19.5 %; meanwhile the yield of liquid products remains relatively stable (~30%). Notably, that at temperatures above 250 °C, the pyrolysis process involves the self-gasification of charcoal by pyrolytic gas. Additionally, the physicochemical and morphological characteristics of the resulting charcoal, including elemental composition, ash content, porosity, and surface structure, are investigated. The results contribute to the systematic understanding of how temperature affects the distribution of pyrolysis products and their properties under fixed-bed conditions and can be applied in the development of energy-efficient and environmentally safe technologies for wood waste utilization.**

***Index Terms*— Biomass, charcoal, fixed-bed reactor, pyrolysis, self-gasification, tar.**

* Corresponding author.
E-mail: badenko@isem.irk.ru

DOI:10.25729/esr.2025.03.0006

Received October 20, 2025. Accepted October 26, 2025. Available online November 28, 2025.

I. Introduction

A key priority in today's research landscape is addressing the reduction in emissions of harmful substances (NO_x, SO_x, etc.) and greenhouse gases (CO_2, H_2O, etc.) from thermal and power generation systems. A highly effective strategy for mitigating these emissions is the integration of biomass resources into the energy balance [1, 2]. According to [3], global biomass consumption for energy production amounts to approximately 1 billion tonnes of oil equivalent, with projections indicating a several-fold increase by 2040. This growth will primarily be driven by the utilization of forestry residues, which are generated annually in vast quantities. As reported in the World Food and Agriculture Statistical Yearbook 2023 [4], 4 billion cubic meters of wood were harvested globally in 2021. Nearly half of this volume, 1.95 billion m³ (equivalent to 410 million tonnes of oil equivalent), was used as biofuel. This biofuel includes residues generated during both the harvesting operations in forests and the wood-processing stages.

Pyrolysis is one of the key thermochemical conversion processes for biomass, and its outcomes strongly depend on process conditions. By adjusting pyrolysis parameters, the process can be steered toward maximizing the yield of liquid products, charcoal, or syngas with tailored characteristics [5, 6]. Among these products, syngas and

TABLE 1. Physicochemical Characteristics of Wood Waste

Proximate analysis (wt%, dry basis)	*Values*
Volatile matter (*VM*)	86.80
Fixed carbon (*FC*)	13.03
Ash content (*AC*)	0.17
Ultimate analysis (wt%, dry basis, ash free)	*Values*
Carbon (*C*)	46.60
Hydrogen (*H*)	6.32
Oxygen (*O**)	47.08
Higher heating value (*Q*, MJ/kg)	18.84
Empirical formula of waste wood	$CH_{1.63}O_{0.76}$

*By difference

charcoal are of particular interest due to their broad applications in energy generation, metallurgy, agriculture, and environmental technologies [7].

Temperature is the critical process parameter governing the yield, composition, and energy properties of pyrolysis products. At lower temperatures (300–700 °C), charcoal formation predominates, yielding a carbon-rich solid with limited degradation of the lignocellulosic structure. As temperature increases (>1100 °C), thermal decomposition of cellulose and hemicellulose intensifies, leading to a higher gas-phase yield, while diminishing the solid residue [8, 9]. Concurrently, the composition of syngas undergoes significant changes: concentrations of H_2, CO, and CH_4 increase, enhancing its heating value and suitability for use in internal combustion engines or fuel cells [10].

Fixed-bed reactors represent one of the most widely used laboratory- and pilot-scale systems for fundamental pyrolysis studies. Their simple design, high reproducibility, and precise temperature control make them an ideal platform for systematically investigating the influence of temperature on product distribution [11].

Despite extensive literature on biomass pyrolysis, gaps remain in the quantitative and qualitative understanding of how product characteristics depend on temperature under fixed-bed conditions, particularly regarding localized heat and mass transfer phenomena specific to this reactor type. Moreover, data correlating pyrolysis temperature with charcoal properties, such as specific surface area, porosity, fixed carbon, and ash content, require further systematic analysis across different biomass types, especially wood waste [12].

This paper aims to determine the optimal pyrolysis parameters for wood chips that maximize process efficiency while minimizing the formation of tar compounds. A series of various experiments were conducted at different pyrolysis temperatures.

II. PROCESS MATERIALS AND EXPERIMENTAL METHOD

A. Feedstock

The study utilized pine wood chips (Pinus silvestris) sized to approximately (30–40) × 10 × 10 mm^3, which were obtained using an electric garden shredder (Viking GE 135). Table 1 presents the details on appearance, as well as proximate and ultimate analysis data. Characteristics of the source wood were determined using standard analytical methods (see section D) and correspond to data obtained by other researchers, for example [13, 14].

B. Laboratory Bench Setup

The laboratory pyrolysis setup for woody biomass (Fig. 1) comprises a reaction chamber, a pyrolysis gas cleaning system, and a tar removal system. The reaction chamber is a fixed-bed thermochemical conversion reactor equipped with a grate (1′), an electrical heating system (1″), thermal insulation (1‴), and thermocouples. The reactor has an internal diameter of 15 cm and a height of 31 cm, with a 5 cm distance between the bottom of the reactor and the grate. The electrical heating system consists of nichrome wire wound around ceramic insulators. Controlled heating is achieved using a voltage regulator and a temperature controller, maintaining precisely the desired pyrolysis temperature. Thermal insulation is provided by fire-resistant glass-ceramic fiber (Cerablanket).

The absence of thermal insulation on the gas outlet pipe facilitates partial condensation of liquid pyrolysis products, which are then returned to the reactor for further cracking.

The reactor is fitted with four Type K thermocouples: the first and second (T1, T2) are positioned within the biomass bed, the third (T3) is located above the bed, and the fourth (T4) measures the temperature of the evolved

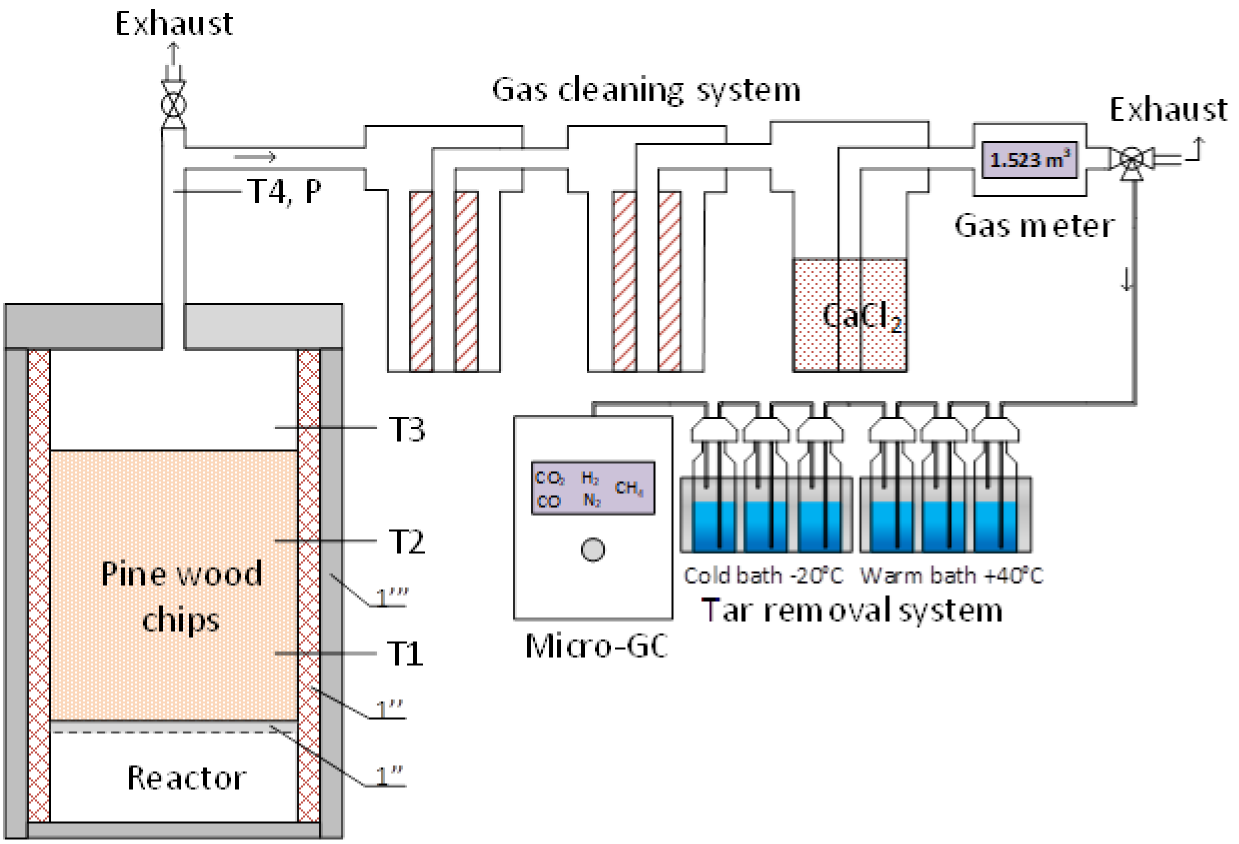

Fig.1 The laboratory bench for pyrolysis of waste wood chips.

gases. Additionally, a differential manometer is installed to monitor pressure drop across the bed. Two relief valves are provided to release excess pressure if necessary.

The gas cleaning system consists of three filters: the first is made of stainless steel, while the second and third are fabricated from transparent polycarbonate. The first two filters are equipped with standard polypropylene foam water filters (PP5-10SL), designed to capture tar and water vapor. The third filter is half-filled with granular calcium chloride ($CaCl_2$) for complete gas drying.

The fine tar removal system follows the method proposed by J.P.A. Neeft and colleagues, as described in [15, 16]. In this approach, syngas passes through a series of impinger bottles filled with isopropanol. Some impingers are immersed in a warm water bath (+40 °C), while others are placed in a cold bath (−20 °C). This technique enables complete tar removal from syngas and is widely adopted by researchers, for example, in [17].

The laboratory setup is also equipped with a gas meter, and the composition of syngas components is analyzed in real time using an INFICON Micro GC Fusion gas chromatograph.

C. Operational Procedures

Approximately (465 ± 1) g of wood waste was loaded into the pyrolysis reactor and gradually heated to the target temperature (360, 400, 440, 480, or 520 °C), which was then maintained constant throughout each experiment. The heating rate was consistent across all tests at approximately

Fig.2 Charcoal agglomerate with tar.

10 °C/min. Upon initiation of pyrolysis, pressure inside the reactor increased, forcing the generated syngas out of the reactor and driving it through the gas duct and subsequent filtration and cleaning systems.

The syngas produced during pyrolysis passes through the layer of charcoal formed in the reactor and then enters an uninsulated gas outlet pipe, which is heated by the hot gas itself. As the gas travels toward the cleaning system, it undergoes reforming. This reforming process reduces tar yield while simultaneously increasing gas yield. As demonstrated in [18], reforming of pyrolytic gas also enhances the hydrogen content in the syngas.

During passage through the gas cleaning system, tar and water vapor are captured, and the gas is fully dried. The cleaned syngas then flows through a gas meter and enters the fine tar removal system before being directed to the gas chromatograph. The INFICON Micro GC Fusion gas chromatograph, operating in online mode, automatically sampled the gas every 3 minutes. It is equipped with Microelectromechanical Systems (MEMS)-based microThermal Conductivity Detectors (TCDs), calibrated to measure the relative concentrations of CO, H_2, CO_2, CH_4, N_2, and hydrocarbons. The total absolute measurement error for all gas components does not exceed 1%.

The experiment was terminated when the gas meter readings stabilized (indicating no further gas evolution) and the excess pressure dropped below the threshold required to transport syngas from the reactor to the chromatograph. Since no external inert gas was supplied to the reactor, the gas meter recorded only the volume of gas generated during wood waste pyrolysis. At the end of each run, heating was switched off, and the reactor was allowed to cool to ambient temperature. The wood charcoal was then extracted.

Char located in the upper part of the reactor formed agglomerates with condensed tar flowing down into the reactor (Fig. 2). Tar was subsequently separated from the char particles using a utility knife and weighed. The mass of the resulting charcoal was also determined. Thereafter, the physicochemical properties and surface morphology of the charcoal were analyzed using scanning electron microscopy (SEM).

The volume of liquid products collected in the gas cleaning system was measured. Tar content was determined by drying a representative liquid sample in a drying oven at 70 °C for 40–50 minutes and weighing the residual solid. This procedure is described in detail in [19]. Subsequently, the elemental composition of the tar was analyzed.

The quantities of tar and water were quantified by measuring the mass difference of the filters before and after drying in an oven at 105 °C. The initial mass of the filters containing both tar and water was recorded immediately after the experiment ended.

D. Analytical Methods

The solid and tar products obtained from the waste wood pyrolysis experiments were characterized using the following analytical methods.

Proximate analysis was performed in accordance with the following ASTM standards:

- ASTM E871 (Standard Test Method for Moisture Analysis of Particulate Wood Fuels),
- ASTM D1102-84(2013) (Standard Test Method for Ash Content (AC) in Wood),
- ASTM E872 (Standard Test Method for Volatile Matter (VM) in the Analysis of Particulate Wood Fuels).

Fixed carbon (*FC*, wt%) was calculated by difference using equation

$$FC = 100 - VM - AC. \quad (1)$$

Ultimate analysis for carbon (*C*, %) and hydrogen (*H*, %) was carried out using a CHNS elemental analyzer (Flash EA 1112, Thermo Finnigan, Italy). The total oxygen (*O*, %) content was determined by difference according to equation

$$O = 100 - AC - C - H. \quad (2)$$

The higher heating value (*Q*, MJ/kg) was calculated from the ultimate analysis data using following equation, originally proposed and validated by Channiwala [20]:

$$Q = 0.3491C + 1.1783H - 0.1034O - 0.0151N - 0.0211AC, \quad (3)$$

where *C, H, S, O, N*, and *AC* represent the mass percentages of carbon, hydrogen, sulfur, oxygen, nitrogen, and ash in the fuel, respectively.

The surface morphology of the pyrolyzed wood samples was examined using scanning electron microscopy (SEM). Chemical microanalysis was performed via energy-dispersive X-ray spectroscopy (EDS) using a Hitachi TM3000 tabletop SEM equipped with an SDD XFlash 430H X-ray detector. Imaging was conducted under low-vacuum conditions (5 kV), which are standard for non-conductive and low-contrast samples. No conductive coating was applied to the samples prior to analysis.

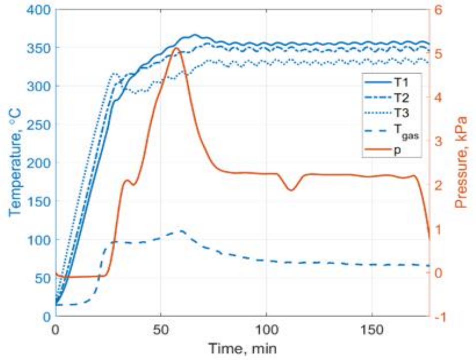

a) 360°C

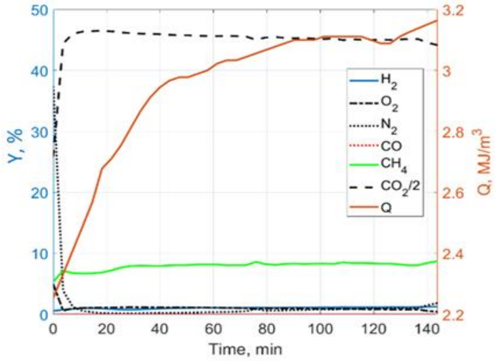

b) 360°C

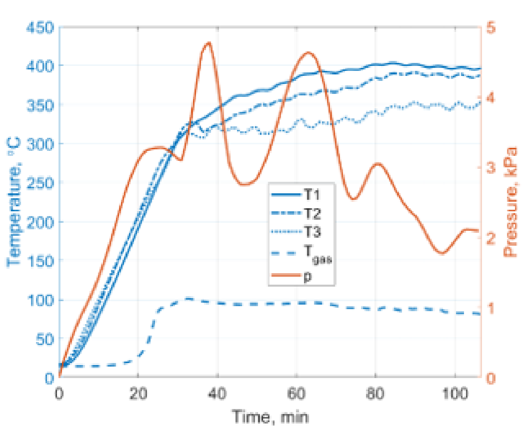

a) 400°C

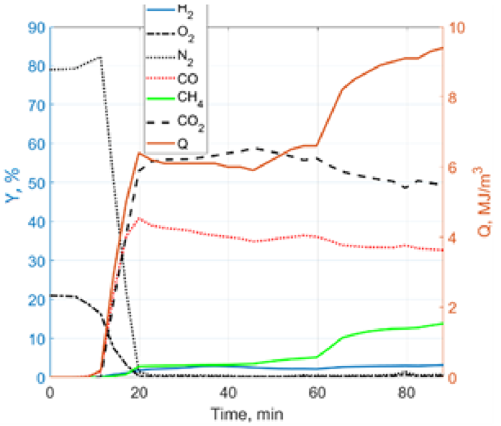

b) 400°C

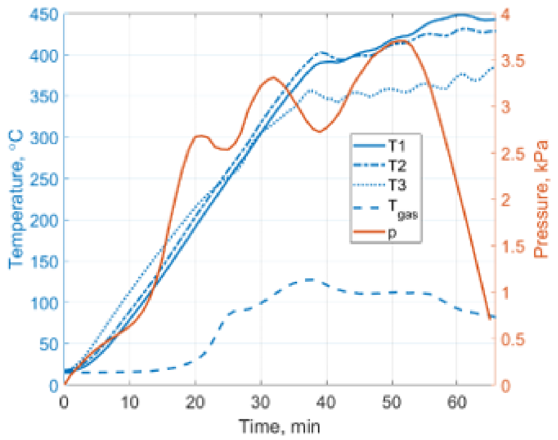

a) 440°C

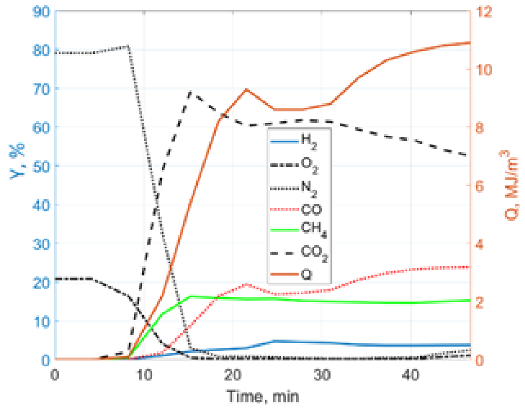

b) 440°C

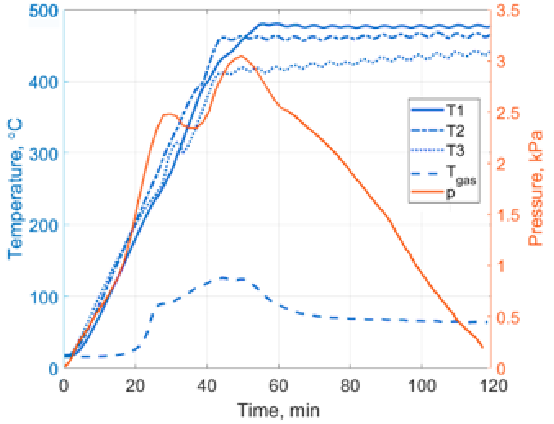

a) 480°C

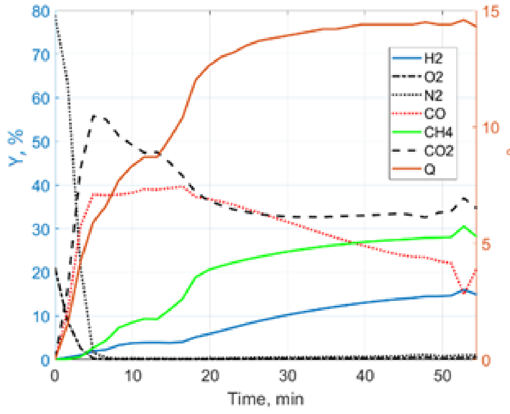

b) 480°C

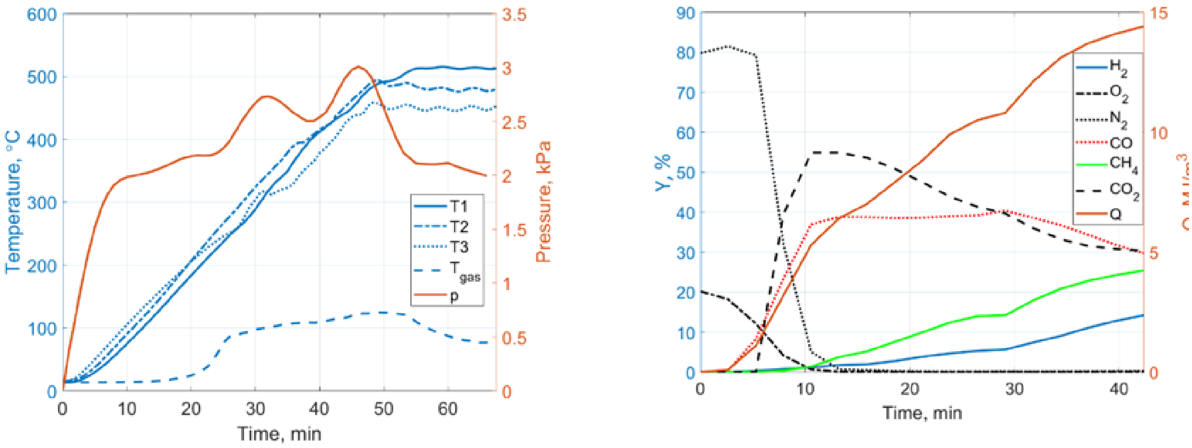

a) 520°C b) 520°C

Fig.3. Profiles of temperature in the bed (T1, T2), above the bed (T3), within fuel and gas (Tgas), as well as pressure curve, depending on the process time (a); Changes in the composition of gas (expressed through the volume fractions Y) and its lower heating value across various pyrolysis temperatures (b).

Pyrolysis of wood chips can be represented by reaction

$$Wood\ chips \rightarrow Char + Liquid\ products\ (tar + water) + Producer\ gas. \quad (4)$$

Based on (4), the yields of pyrolysis products were calculated.

The yields of pyrolysis products Y_j (%) were determined using a mass balance approach according to equation

$$Y_j = \frac{m_j}{m_{wood}} \cdot 100, \quad (5)$$

where m_j and m_{wood} are the masses (kg) of the individual product j (char, liquid, or producer gas) and the initial feedstock, respectively.

Carbon conversion (*CC*) was calculated according to following equation:

$$CC = 1 - \frac{m_{char}\left(y_{CO_2}\frac{12}{44} + y_{CO}\frac{12}{28} + y_{CH_4}\frac{12}{16}\right)}{m_{wood}Y_{char}} \cdot 100, \quad (6)$$

where y_i is the content of components in the producer gas (CO_2, CO, CH_4, H_2). The mechanical gas efficiency (*MGE*) was calculated according to equation

$$MGE = \frac{Q_{gas}}{Q_{wood}} \cdot 100, \quad (7)$$

where Q_{gas} and Q_{wood} are lower heating value of producer gas and wood chips.

The cold gas efficiency (*CGE*) was calculated according to equation

$$CGE = \frac{m_{char}\left(y_{H_2}Q_{H_2} + y_{CO}Q_{CO} + y_{CH_4}Q_{CH_4}\right)}{m_{wood}Q_{wood}} \cdot 100, \quad (8)$$

where Q_i is the heating value of component in the producer gas (CO, CH_4, H_2). The experimental studies were carried out using the resources of the High-Temperature Circuit Multi-Access Research Center at the Melentiev Energy Systems Institute of the Siberian Branch of the Russian Academy of Sciences.

III. Results and Discussion

A. Changes in Producer Gas Composition at Different Temperature

Figure 3a (for pyrolysis temperatures of 360, 400, 440, 480, and 520 °C) presents the time-dependent evolution of temperatures within the biomass bed (T1, T2), above the bed (T3), and in the produced gas (Tgas), as well as the pressure profile during the pyrolysis process. Figure 3b (for the same temperatures) illustrates the variation in composition of syngas (expressed through the volume fractions Y) and its calorific value as a function of pyrolysis temperature.

Analysis of Fig. 3a shows that the initial pressure increase (0–20 min) is caused by thermal expansion of the residual air inside the reactor and by drying of the wood chips, accompanied by evaporation of physically adsorbed moisture. Pyrolysis starts approximately 20 minutes after heating begins, when the temperature within the wood layer reaches 190–210 °C. This is evidenced by a noticeable rise in gas temperature (Tgas), indicating the onset of the active devolatilization phase driven by chemical reactions associated with thermal decomposition.

It is well established that the main macromolecular components of wood undergo thermal decomposition under inert conditions in the following temperature ranges: 225–325 °C for hemicellulose, 305–375 °C for cellulose, and 150–500 °C for lignin [21].

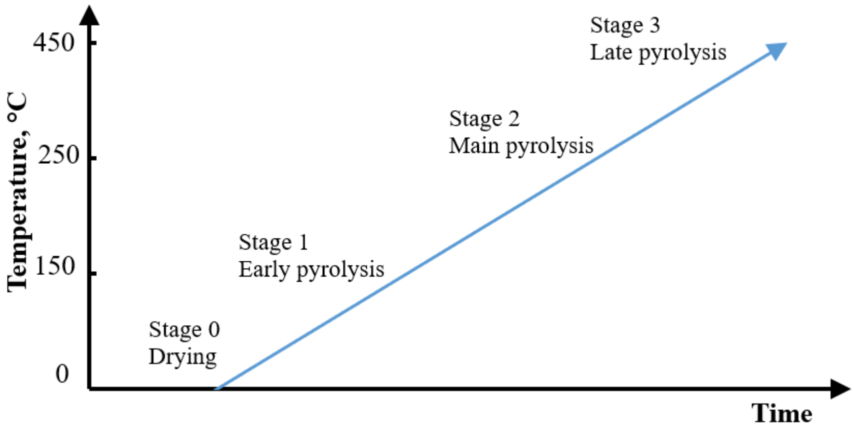

Fig.4. The stages in pyrolysis of wood chips.

TABLE 2. Proximate and Ultimate Analysis of Char Coal

Temperature of pyrolysis, °C	*VM*, %	*AC*, %	*FC*, %	*Q*, MJ/kg	*C*, %	*H*, %	*O*, %	*H/C*	*O/C*
360	36.44	1.07	62.49	31.08	76.53	5.32	18.16	0.83	0.18
400	28.55	1.82	69.63	32.26	80.59	4.82	14.60	0.72	0.14
440	26.71	1.08	72.21	32.80	83.05	4.36	12.60	0.63	0.11
480	16.52	0.95	82.53	34.49	87.34	4.16	8.51	0.57	0.07
520	14.35	1.27	84.38	33.68	92.09	1.85	6.06	0.24	0.05

Analysis of Fig. 3b reveals that the CO_2 concentration in the syngas decreases as pyrolysis temperature rises, while the concentrations of combustible components (CO, CH_4, H_2) and the gas calorific value increase. This trend can be attributed to the self-gasification of char by CO_2 at elevated temperatures, the process described in [22]. Moreover, it is widely accepted that under inert pyrolysis conditions, the oxygen required for CO_2 formation originates primarily from cellulose [23].

It should also be noted that the syngas achieves its maximum calorific value toward the end of the process, which is associated with elevated methane content. Methane is mainly generated from the demethoxylation (–OCH_3) of lignin units in the temperature range of 350 to 450 °C [24].

Carbon monoxide (CO) is produced during thermal decomposition of both cellulose and lignin [23, 25]. As a result, the concentration of CO is relatively stable during the process.

Thus, the pyrolysis process can be described by the scheme presented in Fig. 4:

- Stage 0 (up to 150 °C): Drying of the feedstock.
- Stage 1 (150–250 °C): Initial, low-intensity pyrolysis stage, primarily involving hemicellulose decomposition and formation of light hydrocarbons.
- Stage 2 (250–450 °C): Main pyrolysis stage, characterized by high reaction rates and the generation of the majority of gaseous products. During this stage, residual hemicellulose and cellulose decompose, and lignin degradation begins.
- Stage 3 (>450 °C): Pyrolysis of the remaining, unreacted lignin.

Notably, char self-gasification by CO_2 may occur during both Stage 2 and Stage 3, contributing to the observed increase in H_2 and CO concentrations and the overall enhancement of syngas quality at higher temperatures.

TABLE 3. Ultimate Analysis of Tar

Temperature of pyrolysis, °C	*C*, %	*H*, %	*O*, %
360	53.5	6.7	46.5
400	49.2	6.2	50.8
440	57.1	7.3	42.9
480	51.0	6.7	49.0
520	52.3	5.6	47.7

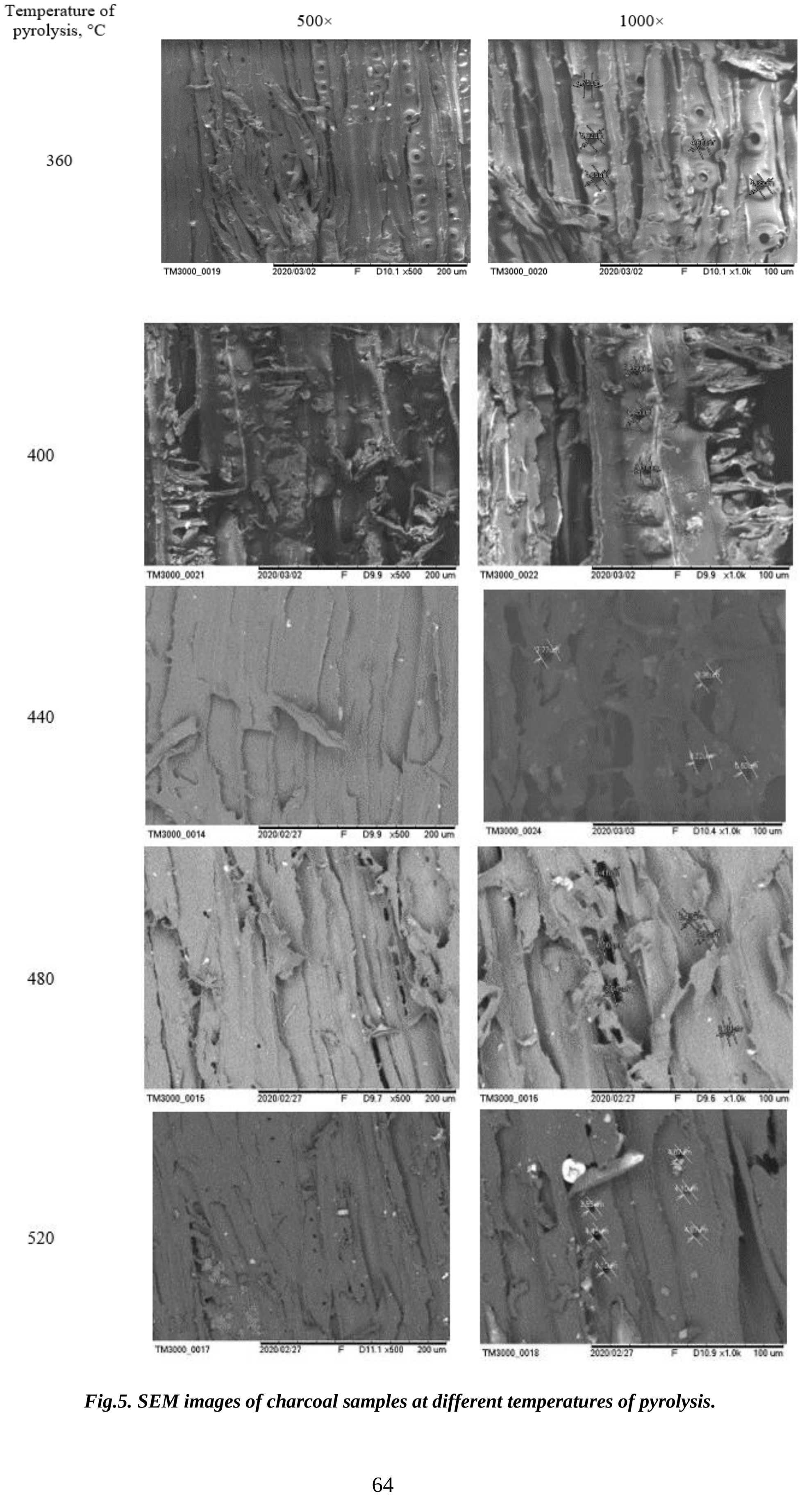

Fig.5. SEM images of charcoal samples at different temperatures of pyrolysis.

B. *Proximate and Ultimate Analysis of Charcoal and Tar*

After each experiment, samples of the produced charcoal were collected and analyzed. The results of the analysis are presented in Table 2.

Proximate analysis includes standard parameters for charcoal: volatile matter (*VM*), ash content (*AC*), and fixed carbon (*FC*). According to Table 2, increasing the pyrolysis temperature resulted in a decrease in volatile matter and a corresponding rise in fixed carbon content. The slight variation in ash content across samples is attributed to the experimental uncertainty inherent in the determination method.

Elevated pyrolysis temperatures led to a reduction in hydrogen (*H*) and oxygen (*O*) content, while carbon (*C*) concentration increased. This trend is explained by two concurrent processes: (i) enhanced carbonization (aromatization and condensation of carbon structures) and (ii) more extensive cleavage of oxygen- and hydrogen-containing functional groups originally present in the wood biopolymers. This progressive deoxygenation and dehydrogenation also account for the observed increase in the higher heating value of the charcoal with rising pyrolysis temperature peaking at 34.49 MJ/kg at 480 °C.

The atomic ratios *H*/*C* and *O*/*C* decrease monotonically with increasing pyrolysis temperature, reflecting the progressive breakdown of polar and aliphatic bonds in the biomass structure. As reported in [26, 27], this decline is also indicative of increasing aromaticity and structural ordering in the charcoal produced at higher temperatures.

Table 3 shows the ultimate analysis of the tar obtained at different temperatures. There is not a clear dependence of the elemental composition on the pyrolysis temperature. The tar is characterized by a high content of oxygen and hydrogen, which can be explained by the fact that the tar contains a large number of chemical compounds, such as aromatic compounds with one to five rings, polycyclic aromatic hydrocarbons, and some oxygen-containing hydrocarbons [28].

C. *Scanning Electron Microscopy Observation*

Figure 5 presents scanning electron microscopy (SEM) images of the surface morphology of wood charcoal samples produced at different pyrolysis temperatures. The images were acquired at magnifications of 500× and 1000×. Higher magnifications resulted in significant charge accumulation on the non-conductive sample surfaces, hindering the acquisition of high-quality images.

For the sample pyrolyzed at 360 °C, a relatively dense fibrous structure largely preserved from the original wood is still evident. This structure is primarily composed of lignin and residual carbohydrates. As the pyrolysis temperature increases, the structure becomes progressively less dense due to partial thermal degradation of lignin. Notably, according to literature data [29–31], complete decomposition of cellulose and hemicellulose in pine wood during pyrolysis occurs at temperatures close to 400 °C.

Microscopic pores formed by the evolution of pyrolysis gases are clearly visible in the samples obtained at 360,

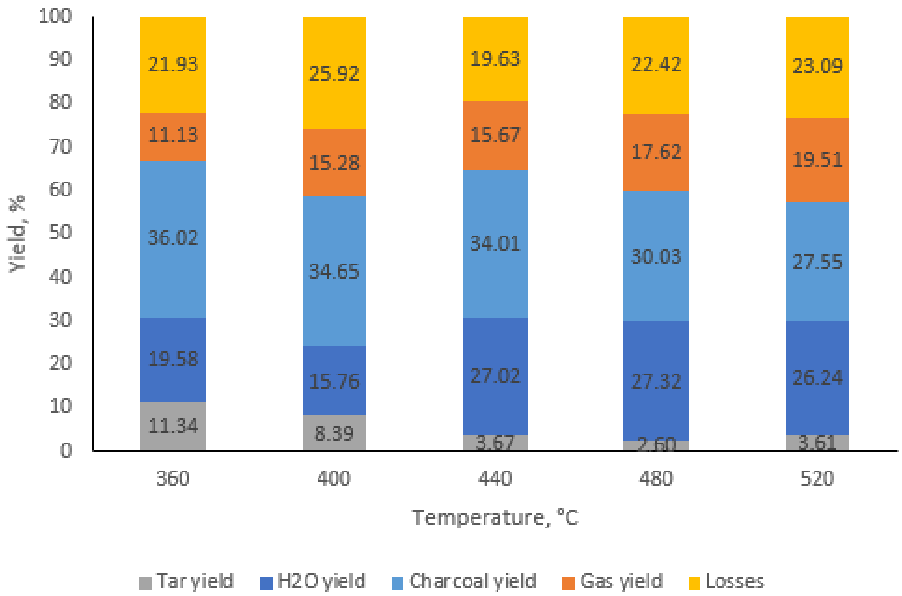

Fig.6. The yields of charcoal, gas, and liquid produced from wood chips at different temperatures.

TABLE 4. Summary of Pyrolysis of Wood Chips at Different Temperatures

Input	Wood chips, kg	0.46				
	Q of wood chips, MJ/kg	18.8				
	Temperature, °C	360	400	440	480	520
Output	[H2], %	1.1	2.6	3.6	9.6	6.7
	[CO], %	0.0	35.5	15.2	30.7	37.0
	[CH4], %	8.1	6.9	19.2	21.7	14.8
	[CO2], %	91.0	54.3	59.8	37.2	41.1
	Q, MJ/m^3	3.0	7.2	9.2	12.7	10.7
	Gas yield, %	11.1	15.3	15.7	17.6	19.5
	Charcoal yield, %	36.0	34.6	34.0	30.0	27.5
	Water yield, %	19.6	15.8	27.0	27.3	26.2
	Tar yield, %	11.3	8.4	3.7	2.6	3.6
	Carbon conversion (*CC*), %	69.4	64.4	63.1	60.0	61.4
	Cold gas efficiency, (*CGE*) %	9.2	19.5	20.7	25.8	20.0
	Mechanical gas efficiency (*MGE*), %	25.9	55.6	61.5	84.9	71.7

400, and 440 °C. The average pore diameter increases with the temperature reaching 4.65–5.32 μm at 360 °C, 5.01–6.45 μm at 400 °C, and 5.62–8.36 μm at 440 °C. In the first two samples (360 °C and 400 °C), these pores are arranged in regular rows aligned with the original fiber orientation. However, this ordered arrangement is no longer discernible at 440 °C due to the progressive breakdown of the fibrous architecture.

At 480 °C, longitudinal fiber fractures appear, with widths ranging from 2.47 to 5.41 μm and varying lengths, resulting in a more developed and irregular surface morphology. Upon further temperature increase to 520 °C, devolatilization is essentially complete, leading to a noticeable reduction in both the number of pores and structural fractures compared to the 480 °C sample.

D. Pyrolysis Efficiency

Figure 6 shows the yields of pyrolysis products as a function of pyrolysis temperature, along with the corresponding mass balance closure error (losses).

With the increasing pyrolysis temperature, the charcoal yield decreases from 36% to 27.5%, while the syngas yield rises from 11.1% to 19.5%. In contrast, the liquid product yield remains relatively constant at approximately 30% across most temperatures, with the exception of the run conducted at 400 °C, where it drops to 24.2%. This deviation is attributed to experimental uncertainties in accurately quantifying the liquid fraction particularly due to collection losses, adhesion to system surfaces, and incomplete separation of tar from water.

The same uncertainty in liquid product measurement is the primary contributor to the observed mass balance discrepancy, which amounts to approximately 22%. This unaccounted fraction likely includes unrecovered condensable vapors, aerosolized tars retained in the gas lines, and minor measurement errors in solid and gas quantification.

Table 4 summarizes the key results of wood chip pyrolysis as a function of temperature. The syngas composition shown in Fig. 3b is averaged over the period after residual air has been fully purged from the reactor. Analysis of the gas composition reveals that the concentration of combustible components (H_2, CO, CH_4) increases with rising pyrolysis temperature, although the relative distribution among these components varies non-uniformly.

The findings indicate that the pyrolysis temperature of 480 °C is optimal, resulting in the maximum lower heating value of syngas (12.7 MJ/m³) and consequently the highest values of Mechanical Gas Efficiency (*MGE*) and Cold Gas Efficiency (*CGE*), which reach 84.9% and 25.8%, respectively.

Analysis of *MGE* and *CGE* trends shows that both efficiencies improve as temperatures climb to 480 °C, but then decline at 520 °C. The relatively low CGE values across all tests are attributed to the inherent energy inefficiency of the laboratory-scale pyrolysis setup, primarily due to significant heat losses to the environment.

Notably, the lowest efficiency values were observed at 360 °C, despite this run exhibiting the highest carbon conversion (69.4%). This apparent contradiction arises because, at this low temperature, the pyrolysis reactions proceed slowly and with low intensity, requiring the longest residence time of the feedstock in the reactor to achieve near-complete carbon conversion. In contrast, at the optimal temperature of 480 °C, carbon conversion is slightly lower (60%) but occurs more rapidly and produces a syngas of significantly higher energy quality, resulting in superior overall process efficiency.

IV. Conclusion

The paper proposes a novel fixed-bed reactor concept designed to minimize tar formation while simultaneously enhancing syngas yield. The reactor's performance was investigated across a range of pyrolysis temperatures, including 360, 400, 440, 480, and 520 °C. The findings demonstrate that 480 °C is the optimal pyrolysis temperature, resulting in the highest syngas heating value (12.69 MJ/m^3) and peak efficiency metrics: a Mechanical Gas Efficiency of 84.9% and a Cold Gas Efficiency of 25.8%.

The study has established that as pyrolysis temperature increases, the solid char yield decreases from 36% to 27.5%, while syngas yield rises from 11.1% to 19.5%. In contrast, the liquid product yield remains relatively stable at approximately 30%, with the exception of the 400 °C run, where it dropped to 24.2%, likely due to experimental uncertainties in liquid collection and quantification. The overall mass balance closure error of approximately 22% is primarily attributed to unmeasured condensable vapors, tar deposition in gas lines, and minor measurement inaccuracies.

Additionally, the physicochemical properties and surface morphology of the resulting wood charcoal are characterized, offering valuable insights into structural transformation across various temperatures. These findings contribute to the development of energy-efficient, low-tar pyrolysis technologies for sustainable wood waste valorization.

Acknowledgment

The research was funded by the Russian Science Foundation, Grant No. 24-29-00596 (https://rscf.ru/project/24-29-00596/).

References

[1] J. Popp, Z. Lakner, M. Harangi-Rákos, M. Fári, "The effect of bioenergy expansion: Food, energy, and environment," Renewable and Sustainable Energy Reviews, vol. 32, pp. 559–578, 2014. DOI: 10.1016/j.rser.2014.01.056.

[2] Y. Kang, Q. Yang, P. Bartocci, H. Wei, S. S. Liu, Z. Wu, H. Zhou, H. Yang, F. Fantozzi, H. Chen, "Bioenergy in China: Evaluation of domestic biomass resources and the associated greenhouse gas mitigation potentials," Renewable and Sustainable Energy Reviews, vol. 127, Art. no. 109842, 2020. DOI: 10.1016/j.rser.2020.109842.

[3] M. S. Roni, S. Chowdhury, S. Mamun, M. Marufuzzaman, W. Lein, S. Johnson, "Biomass co-firing technology with policies, challenges, and opportunities: A global review," Renewable and Sustainable Energy Reviews, vol. 78, pp. 1089–1101, 2017. DOI: 10.1016/j.rser.2017.05.023.

[4] "World food and agriculture – statistical yearbook 2023," FAOSTAT, 2023. [Online] Available: https://openknowledge.fao.org/server/api/core/bitstreams/6e04f2b4-82fc-4740-8cd5-9b66f5335239/content. Accessed on: Jun. 07, 2025.

[5] X. Hu, M. Gholizadeh, "Biomass pyrolysis: A review of the process development and challenges from initial researches up to the commercialisation stage," Journal of Energy Chemistry, vol. 39, pp. 109–143, 2019. DOI: 10.1016/j.jechem.2019.01.024.

[6] J. R. Lesme, F. R. M. Nascimento, O. J. Venturini, E. E. S. Lora, "Chapter Five – Biomass energy conversion: Routes and products," in From Crops and Wastes to Bioenergy, Woodhead Publishing, 2025, ch. 5, pp. 139–190. DOI: 10.1016/B978-0-443-16084-4.00018-3.

[7] A. de Oliveira Vilela, E. S. Lora, Q. R. Quintero, R. A. Vicintin, T. Pacceli da Silva e Souza, "A new technology for the combined production of charcoal and electricity through cogeneration," Biomass and Bioenergy, vol. 69, pp. 222–240, 2014. DOI: 10.1016/j.biombioe.2014.06.019.

[8] J. Li, K. Xu, X. Yao, J. Liu, "Investigation of biomass slow pyrolysis mechanisms based on the generation trends in pyrolysis products," Process Safety and Environmental Protection, vol. 183, pp. 327–338, 2024. DOI: 10.1016/j.psep.2024.01.027.

[9] A. Gao, K. Zou, Y. Wang, G. Gao, M. V. Penzik, A. N. Kozlov, Y. M. Isa, Y. Huang, S. Zhang, "The core factors in determining product distributions during pyrolysis: The synergistic effect of volatile-char interactions and temperature," Renewable Energy, vol. 218, Art. no. 119359, 2023. DOI: 10.1016/j.renene.2023.119359.

[10] N. Ungureanu, N.-V. Vladut, S.-S. Biris, N.-E. Gheorg, M. Ionescu, “Biomass Pyrolysis Pathways for Renewable Energy and Sustainable Resource Recovery: A Critical Review of Processes, Parameters, and Product Valorization,” Sustainability, vol. 17, no. 17, 2025. DOI: 10.3390/su17177806.

[11] M. Alam, I. Sarkar, N. Chanda, S. Ghosh, C. Loha, “Enhancing syngas production and hydrogen content in syngas from catalytic slow pyrolysis of biomass in a pilot scale fixed bed reactor,” Biomass Conversion and Biorefinery, vol. 15, no. 4, pp. 6237-6249, 2025. DOI: 10.1007/s13399-024-05453-0.

[12] F. Mahmood, M. Ali, M. Khan, C. F. Mbeugang, Y. M. Isa, A. Kozlov, M. Penzik, X. Xie, H. Yang, S. Zhang, B. Li, “A review of biochar production and its employment in synthesizing carbon-based materials for supercapacitors,” Industrial Crops and Products, vol. 227, Art. no. 120830, 2025. DOI: 10.1016/j.indcrop.2025.120830.

[13] Z. Sun, B. Xu, A. H. Rony, S. Toan, S. Chen, K. A. M. Gasem, H. Adidharma, M. Fan, W. Xiang, “Thermogravimetric and kinetics investigation of pine wood pyrolysis catalyzed with alkali-treated CaO/ZSM-5,” Energy Conversion and Management, vol. 146, pp. 182–194, 2017. DOI: 10.1016/j.enconman.2017.04.104.

[14] K. H. Kim, J.-Y. Kim, T.-S. Cho, J. W. Choi, “Influence of pyrolysis temperature on physicochemical properties of biochar obtained from the fast pyrolysis of pitch pine (Pinus rigida),” Bioresource Technology, vol. 118, pp. 158–162, 2012. DOI: 10.1016/j.biortech.2012.04.094.

[15] J. P. A. Neeft, H. A. M. Knoef, U. Zielke, K. Sjostrom, P. Hasler, P. A. Simell, M.A. Dorrington, L. Thomas, N. Abatzoglou, S. Deutch, “Guideline for sampling and analysis of tar and particles in biomass producer gases,” Progress in thermochemical biomass conversion, vol. 1, pp. 162–175, 2001.

[16] J. P. A. Neeft, “Tar Guideline: A standard method for measurement of tars and particles in biomass producer gases,” in Proc. 12th EUBCE, Amsterdam, Netherlands, 2002, pp. 469–472.

[17] T. Sharma, D. M. Yepes Maya, F. R. M. Nascimento, Y. Shi, A. Ratner, E. E. Silva Lora, L. J. Mendes Neto, J. C. Escobar Palacios, R. Vieira Andrade, “An Experimental and Theoretical Study of the Gasification of Miscanthus Briquettes in a Double-Stage Downdraft Gasifier: Syngas, Tar, and Biochar Characterization,” Energies, vol. 11, no. 11, Art. no. 3225, 2018. DOI: 10.3390/en11113225.

[18] K. Shi, J. Yan, J. A. Menendez, X. Luo, G. Yang, Y. Chen, E. Lester, T. Wu, “Production of H2-Rich Syngas From Lignocellulosic Biomass Using Microwave-Assisted Pyrolysis Coupled With Activated Carbon Enabled Reforming,” Frontiers in Chemistry, vol. 8, 2020. DOI: 10.3389/fchem.2020.00003.

[19] D. A. Svishchev, A. N. Kozlov, I. G. Donskoy, A. F. Ryzhkov, “A semi-empirical approach to the thermodynamic analysis of downdraft gasification,” Fuel, vol. 168, pp. 91–106, 2016. DOI: 10.1016/j.fuel.2015.11.066.

[20] S. A. Channiwala, P. P. Parikh, “A unified correlation for estimating HHV of solid, liquid and gaseous fuels,” Fuel, vol. 81, no. 8, pp. 1051–1063, 2002. DOI: 10.1016/S0016-2361(01)00131-4.

[21] N. Labbe, L. M. Kline, L. Moens, K. Kim, P. C. Kim, D. G. Hayes, “Activation of lignocellulosic biomass by ionic liquid for biorefinery fractionation,” Bioresource Technology, vol. 104, pp. 701–707, 2012. DOI: 10.1016/j.biortech.2011.10.062.

[22] A. Dominguez, Y. Fernandez, B. Fidalgo, J. J. Pis, J. A. Menendez, “Bio-syngas production with low concentrations of CO2 and CH4 from microwave-induced pyrolysis of wet and dried sewage sludge,” Chemosphere, vol. 70, no. 3, pp. 397–403, 2008. DOI: 10.1016/j.chemosphere.2007.06.075.

[23] R. Laryea-Goldsmith, C. Woolard, “Thermal with Mass Spectroscopic Analysis of Wood and Cereal Biomass Torrefaction,” International Scholarly Research Notices, no. 1, Art. no. 508965, 2013.

[24] E. Jakab, O. Faix, F. Till, “Thermal decomposition of milled wood lignins studied by thermogravimetry/mass spectrometry,” Journal of Analytical and Applied Pyrolysis, vol. 40–41, pp. 171–186, 1997. DOI: 10.1016/S0165-2370(97)00046-6.

[25] Y. Chen, J. Duan, Y. Luo, “Investigation of agricultural residues pyrolysis behavior under inert and oxidative conditions,” Journal of Analytical and Applied Pyrolysis, vol. 83, no. 2, pp. 165–174, 2008. DOI: 10.1016/j.jaap.2008.07.008.

[26] S. Wei, M. Zhu, X. Fan, J. Song, P. Peng, K. Li, W. Jia, H. Song, “Influence of pyrolysis temperature and feedstock on carbon fractions of biochar produced from pyrolysis of rice straw, pine wood, pig manure and sewage sludge,” Chemosphere, vol. 218, pp. 624–631, 2019. DOI: 10.1016/j.chemosphere.2018.11.177.

[27] S. Li, S. Harris, A. Anandhi, G. Chen, “Predicting biochar properties and functions based on feedstock and pyrolysis temperature: A review and data syntheses,” Journal of Cleaner Production, vol. 215, pp. 890–902, 2019. DOI: 10.1016/j.jclepro.2019.01.106.

[28] F. Guo, X. Jia, S. Liang, N. Zhou, P. Chen, R. Ruan, “Development of biochar-based nanocatalysts for tar cracking/reforming during biomass pyrolysis and gasification,” Bioresource Technology, vol. 298, Art. no. 122263, 2020. DOI: 10.1016/j.biortech.2019.122263.

[29] X. Hu, H. Guo, M. Gholizadeh, B. Sattari, Q. Liu, “Pyrolysis of different wood species: Impacts of C/H ratio in feedstock on distribution of pyrolysis products,” Biomass and Bioenergy, vol. 120, pp. 28–39, 2019. DOI: 10.1016/j.biombioe.2018.10.021.

[30] C.H. Pang, E. Lester, T. Wu, “Influence of lignocellulose and plant cell walls on biomass char morphology and combustion reactivity,” Biomass and Bioenergy, vol. 119, pp. 480–491, 2018. DOI: 10.1016/j.biombioe.2018.10.011.

[31] W. Cai, R. Liu, “Performance of a commercial-scale biomass fast pyrolysis plant for bio-oil production,” Fuel, vol. 182, pp. 677–686, 2016. DOI: 10.1016/j.fuel.2016.06.030.

Vladislav Badenko is a Junior Researcher in the Department of Thermal Power Systems at the Melentiev Energy Systems Institute of the Siberian Branch of the Russian Academy of Sciences (ESI SB RAS). His research interests include thermochemical conversion of biomass, numerical modeling of combustion processes, and combined energy facilities for biomass decomposition.

Maxim Penzik, Ph.D., is a Senior Researcher in the Department of Thermal Power Systems at the ESI SB RAS. Since 2022, he has been an Associate Professor at the Faculty of Chemistry at Irkutsk State University. His research interests include the study on the processes of thermal decomposition of biomass, polymers, and organic compounds using the TG-MS method.

Elena V. Gubiy, Ph.D., is a Research Associate in the Department for Complex and Regional Energy Problems at the ESI SB RAS. Her research interests include the analysis of the efficiency of biofuels and the assessment of the bioenergy expansion potential.

Alexander Kozlov, Ph.D., is a Senior Researcher in the Department of Thermal Power Systems at the ESI SB RAS. His research interests include the combustion of heterogeneous solid fuels (biomass, coal) and the development of simple engineering techniques for calculating gasification processes.